Translational Oncology 26 (2022) 101533

Contents lists available at ScienceDirect

Translational Oncology

journal homepage: www.elsevier.com/locate/tranon

Original Research

Thrombospondin-1 overexpression stimulates loss of Smad4 and accelerates malignant behavior via TGF-β signal activation in pancreatic ductal adenocarcinoma

Kazuki Matsumura, Hiromitsu Hayashi, Norio Uemura, Yoko Ogata, Liu Zhao, Hiroki Sato, Yuta Shiraishi, Hideyuki Kuroki, Fumimasa Kitamura, Takayoshi Kaida, Takaaki Higashi, Shigeki Nakagawa, Kosuke Mima, Katsunori Imai, Yo-ichi Yamashita, Hideo Baba *

Department of Gastroenterological Surgery, Graduate School of Life Sciences, Kumamoto University, 1-1-1 Honjo, Kumamoto 860-8556, Japan

ARTICLE INFO

Keywords:
Cancer associated fibroblasts
Pancreatic ductal adenocarcinoma
Smad4
Stiffness
Thrombospondin-1

ABSTRACT

Introduction: Pancreatic ductal adenocarcinoma (PDAC) is characterized by abundant stroma and cancer-associated fibroblasts (CAFs) provide a favorable tumor microenvironment. Smad4 is known as tumor suppressor in several types of cancers including PDAC, and loss of Smad4 triggers accelerated cell invasiveness and metastatic potential. The thrombospondin-1 (TSP-1) can act as a major activator of latent transforming growth factor-β (TGF-β) in vivo. However, the roles of TSP-1 and the mediator of Smad4 loss and TGF-β signal activation during PDAC progression have not yet been addressed. The aim is to elucidate the biological role of TSP-1 in PDAC progression.

Methods and results: High substrate stiffness stimulated TSP-1 expression in CAFs, and *TSP-1* knockdown inhibited cell proliferation with suppressed profibrogenic and activated stroma-related gene expressions in CAFs. Paracrine TSP-1 treatment for PDAC cells promoted cell proliferation and epithelial mesenchymal transition (EMT) with activated TGF-β signals such as phosphorylated Akt and Smad2/3 expressions. Surprisingly, knockdown of *DPC4* (Smad4 gene) induced TSP-1 overexpression with TGF-β signal activation in PDAC cells. Interestingly, TSP-1 overexpression also induced downregulation of Smad4 expression and enhanced cell proliferation in vitro and in vivo. Treatment with LSKL peptide, which antagonizes TSP-1-mediated latent TGF-β activation, attenuated cell proliferation, migration and chemoresistance with enhanced apoptosis in PDAC cells.

Conclusions: TSP-1 derived from CAFs stimulates loss of Smad4 expression in cancer cells and accelerates malignant behavior by TGF-β signal activation in PDAC. TSP-1 could be a novel therapeutic target, not only for CAFs in stiff stroma, but also for cancer cells in the PDAC microenvironment.

Introduction

Pancreatic ductal adenocarcinoma (PDAC) displays aggressive malignant behavior and is the most lethal cancer type worldwide [1]. PDAC is characterized by abundant stroma that harbors tumor-promoting properties and chemoresistance. The hard and fibrotic shell of desmoplasia serves as a barrier to the infiltration of both chemo- and immunotherapy drugs and host immune cells to the tumor [2]. The stromal component of PDAC occupies up to 80% of the tumor mass and causes PDAC to become one of the stiffest malignancies with solid stress values close to 10 kPa [3].

In many solid cancers, the dense stroma is predominantly composed of cancer-associated fibroblasts (CAFs), as well as macrophages, immune cells, endothelial cells, and epithelial cells [4]. Epithelial mesenchymal

Abbreviations: CAFs, cancer associated fibroblasts; CTGF, connective tissue growth factor; DAB, diaminobenzidine; DAPI, 4',6-diamidino-2-phenylindole; EMT, epithelial mesenchymal transition; FBS, fetal bovine serum; IHC, immunohistochemistry; LAP, latency-associated peptide; NFs, normal fibroblasts; OS, overall survival; L-OHP, oxaliplatin; PDAC, pancreatic ductal adenocarcinoma; PBS, phosphate-buffered saline; qRT-PCR, quantitative reverse transcription polymerase chain reaction; RFS, recurrence free survival; rTSP-1, recombinant TSP-1; RPMI, Roswell Park Memorial Institute; SD, standard deviation; siRNA, small interfering RNA; TSP-1, thrombospondin-1; TGF-β, transforming growth factor-β.

* Corresponding author.
E-mail address: hdobaba@kumamoto-u.ac.jp (H. Baba).

https://doi.org/10.1016/j.tranon.2022.101533
Received 29 April 2022; Received in revised form 3 September 2022; Accepted 5 September 2022

transition (EMT) is a process of cellular plasticity that contributes to cancer cell invasion and metastasis [5], and CAFs can promote EMT in cancer cells [6]. CAFs also produce various paracrine molecules such as transforming growth factor-β (TGF-β) that aid tumor growth, local invasion, and metastases development for cancer cells.

TGF-β is a potent inducer of EMT [7], and TGF-β signaling has a central role in the tumor progression of multiple cancers, including PDAC [8]. Smad4 plays a pivotal role in the signal transduction of the TGF-β superfamily cytokines by mediating transcriptional activation of target genes [9]. Smad4 is known as a tumor suppressor in several cancer types such as PDAC, colorectal cancer, intrahepatic cholangiocarcinoma, and prostate cancer, and loss of Smad4 triggers accelerated cell invasiveness and metastatic potential [10–16]. In patients with resectable PDAC, loss of Smad4 immunolabeling was an independent poor prognostic factor for overall survival (OS) and disease-free survival [12], and all patients who achieved 5-year survival displayed intact Smad4 expression [12]. Furthermore, PDAC patients with biallelic deletion of *DPC4* (Smad4 gene) had more frequent metastasis compared with those with wild-type *DPC4* [17]. Thus, the inactivation and/or downregulation of Smad4 plays a critical role in PDAC progression. However, the mediator of Smad4 loss and TGF-β signal activation during PDAC progression is unknown.

The matricellular protein thrombospondin-1 (TSP-1) (encoded by *THBS1*) was first demonstrated as a component of the α-granule in platelets and is induced in response to tissue damage or stress, playing a role as a transient component of the extracellular matrix during tissue repair [18–20]. TSP-1 can convert latent TGF-β1 complexes to their biologically active form [21,22]. Because TGF-β is synthesized as a latent complex consisting of latency-associated peptide (LAP), an important step in the regulation of its biological activity is the conversion of the latent form to the active form in vivo [21]. However, the roles of TSP-1 and the mediator of Smad4 loss and TGF-β signal activation during PDAC progression have not yet been addressed.

Here, we investigated the biological role of TSP-1 in PDAC progression. Then, we identified that TSP-1 derived by CAFs stimulates the loss of Smad4 expression in cancer cells accelerating malignant behavior via TGF-β signal activation in PDAC.

Materials and methods

Cell lines and culture conditions

Human pancreatic cancer cell lines (AsPC-1, KLM-1, MIA PaCa-2, PANC-1, PK-59, PK-8, S2-013, and S2-VP10) were used. AsPC-1, KLM-1, PANC-1, PK-59, and PK-8 were cultured in Roswell Park Memorial Institute (RPMI) 1640 supplemented with 10% fetal bovine serum (FBS). MIA PaCa-2, S2-013, and S2-VP10 were cultured in Dulbecco's Modified Eagle's Medium (4.5 g/L glucose) supplemented with 10% FBS. All cell lines were maintained at 37°C in a humidified atmosphere of 5% CO_2.

Establishment of CAFs and NFs

Establishment of CAFs and normal fibroblasts (NFs) was performed as previously described [23]. Patient-derived material was obtained from pancreas resections (pancreatoduodenectomy or distal pancreatectomy) of primary cancers. CAFs were extracted from pancreatic cancer tissues, and paired NFs were extracted from noncancerous tissues using a scalpel. NFs were collected at least 5 cm away from the cancerous region. The tissues were transferred to culture medium and placed on ice. Using scalpels, each material was minced into small pieces that were approximately 2–4 mm in size. After mincing, the tissue pieces were transferred into a gentleMACS C tube containing the enzyme mix by gently adding 4.7 ml RPMI 1640, 200 ml Enzyme H, 100 ml Enzyme R, and 25 ml Enzyme A. The tissue was dispersed and disrupted using the gentleMACS Dissociator. A short centrifugation was performed at 300 × g for 30 s at room temperature (22°C–25°C) to collect the sample materials at the bottom of the tube. The pellet was washed with 20 ml RPMI 1640 to collect any remaining cells lodged in the cell strainer. The cell suspension was then centrifuged at 300 x g at 4°C for 7 min and the supernatant was completely aspirated. The cells were cultured in a 10 cm collagen-coated dish in 10 ml culture media in a 37°C incubator with 5% CO_2 and 95% humidity, and were expanded until they reached a confluency of 90% in a 15 cm dish.

RNA extraction and quantitative reverse transcription PCR

Total RNA extraction, cDNA synthesis, and quantitative reverse transcription polymerase chain reaction (qRT-PCR) were performed as previously described [20, 24]. See Supplementary materials and methods for additional details.

Protein sample preparation and western blot analysis

Protein extractions from cultivated cells and subsequent western blot analyses were performed as previously described [20,24]. Briefly, whole cell lysates from cell lines or 50 mg protein were prepared in RIPA buffer [25 mM Tris-HCl (pH 7.6), 150 mM NaCl, 1% NP-40, 1% sodium deoxycholate, 0.1% SDS] containing protease and phosphatase inhibitors. Equal amounts of protein from cell lysates were electrophoretically separated on 10%–15% sodium dodecyl sulfate gels and transferred onto polyvinylidene fluoride membranes (Bio-Rad, Hercules, CA, USA). The membranes were blocked with 5% non-fat dry milk in TBS/Tween-20 (0.1%) for 1 h at room temperature, followed by incubation with a primary antibody in Can Get Signal Solution 1 (Toyobo) at 4°C overnight. After washing the membrane with TBS/Tween-20, the membranes were incubated with a horseradish peroxidase-conjugated secondary antibody in Can Get Signal Solution 2 at room temperature for 1 h. The membranes were washed with TBS/Tween-20, incubated with an Enhanced Chemiluminescence Detection System [ECL (GE Healthcare Corp) or ECL-Prime (GE Healthcare)], and visualized using a ChemiDoc™ Touch Gel Imaging System (Bio-Rad). Quantification of band intensities for each represented blot was performed using ImageJ (NIH, USA) (Fig. S1).

Immunohistochemical and immunofluorescence staining

Sample processing and immunohistochemical procedures were performed as described previously [20,24]. Briefly, immunohistochemical staining was performed on 4-μm-thick sections from formalin-fixed, paraffin-embedded blocks. Sections were microwave-pretreated in Histofine antigen retrieval solution (pH 9) (Nichirei, Tokyo, Japan). Endogenous peroxidase activity was blocked with 3% hydrogen peroxide, and the sections were incubated with diluted antibodies overnight at 4°C. A subsequent reaction was performed with a biotin-free horseradish peroxidase enzyme-labeled polymer from the Envision Plus detection system (Dako Co. Tokyo, Japan). A positive reaction was visualized with diaminobenzidine (DAB) solution, followed by counterstaining with Mayer's hematoxylin. Negative control for immunostaining was prepared by omitting the primary antibody. For immunofluorescence staining, cells were fixed for 10 min with ice-cold 4% PFA. After being blocked with 3% BSA (Sigma) in phosphate-buffered saline (PBS), cells were permeabilized with 0.2% Triton X-100 and incubated with primary antibody in 3% BSA in PBS and phalloidin overnight, followed by secondary antibody labeled with Alexa Fluor 488 (1:200). After being washed twice with PBS, the nuclei were stained with 4,6-diamidino-2-phenylindole (DAPI). Negative control staining was performed by omitting the primary antibody. The slides were visualized using a BZ-X710 microscope (Keyence).

Immunohistochemical analysis of the expression in cancer stroma and cells (TSP-1 and LAP) was performed by a two-way system using staining intensity and extent. Staining intensity was graded as 0 (negative), 1 (weak), 2 (moderate) and 3 (strong); staining extent was graded

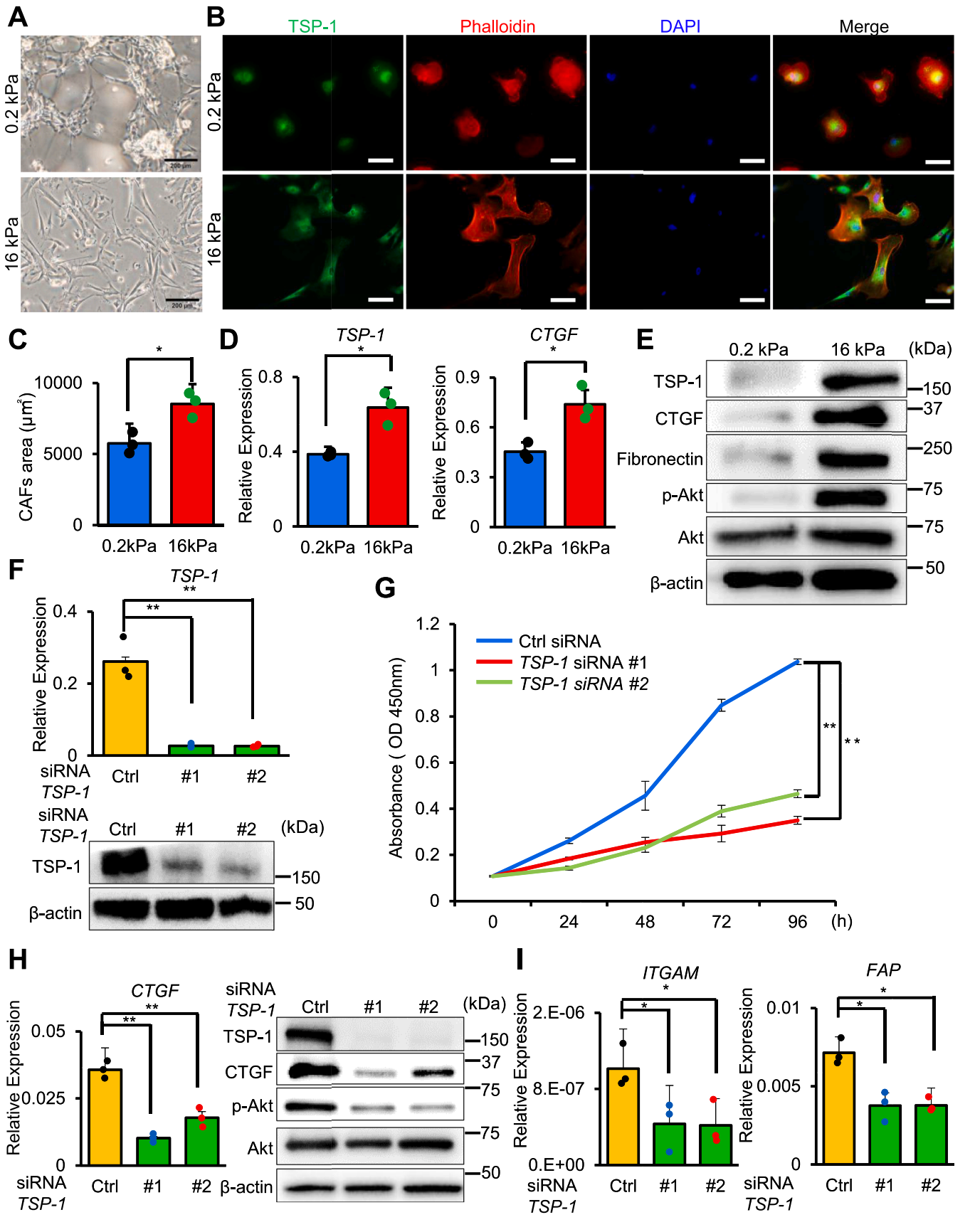

(caption on next page)

Fig. 1. *Stiffness stimulates TSP-1 expression in CAFs, and the downregulation of TSP-1 hinders cell proliferation with suppressed profibrogenic response*. A Cell morphology of CAFs cultured on 0.2 kPa and 16 kPa substrate stiffness. Representative images are shown. B Immunofluorescence staining of TSP-1 (green)/phalloidin (red)/4',6-diamidino-2-phenylindole (DAPI, blue) in CAFs cultured on 0.2 kPa and 16 kPa for 24 h. C The area of CAFs cultured on 0.2 kPa and 16 kPa substrate stiffness was quantified by the phalloidin-/actin-positive area ($^*P < 0.05$; $n = 3$). D qRT-PCR analysis of *TSP-1* and *CTGF* mRNA expression in CAFs cultured on 0.2 kPa and 16 kPa for 24 h. Data were normalized to the amount of *β-actin* mRNA serving as the internal control ($^*P < 0.05$; $n = 3$). E Western blot analysis of TSP-1, CTGF, Fibronectin, and phosphorylation of Akt in CAFs cultured on 0.2 kPa and 16 kPa for 24 h. β-actin served as a loading control ($n = 3$). F *TSP-1* knockdown using siRNA was performed in CAFs. qRT-PCR and western blot analysis were performed in CAFs cultured on conventional 0.5% gelatin coated 100 mm dish for 48 h after *TSP-1* knockdown ($^{**}P < 0.01$; $n = 3$). G Cell proliferation assay in CAFs cultured on conventional 0.5% gelatin coated 100mm dish with *TSP-1* knockdown was performed ($^{**}P < 0.01$; $n = 3$). H Left panel) *TSP-1* knockdown downregulated *CTGF* mRNA levels in CAFs cultured on conventional 0.5% gelatin coated 100 mm dish. Right panel) *TSP-1* knockdown decreased CTGF expression and phosphorylation of Akt in CAFs. Representative blots are shown. qRT-PCR and western blot analyses were performed at 48 h after *TSP-1* knockdown ($^{**}P < 0.01$; $n = 3$). I Suppression of activated stroma subtype-related genes (*ITGAM* and *FAP*) by *TSP-1* knockdown. qRT-PCR was performed in CAFs cultured on conventional 0.5% gelatin coated 100 mm dish for 48 h after *TSP-1* knockdown in CAFs ($^*P < 0.05$; $n = 3$).

as 0 (0%–4%), 1 (5%–24%), 2 (25%–49%), 3 (50%–74%) and 4 (>75%). Values of the intensity and the extent were multiplied as an IHC score. The expression was graded as low (scores, 0–4) and high (scores, 6–12) [25]. Immunohistochemical labeling of Smad4 was scored as intact (positive), which indicated the presence of an intact gene, or lost (negative), which indicated a loss of function mutation or deletion of the gene [26,27]. Blinded samples were evaluated by two observers (KM and NU). During subsequent evaluating, any confusing cases were discussed by the two observers and determined the expression.

Antibodies and reagents

The primary antibodies and reagents used in this study were listed in Supplemental materials and methods.

TSP-1 and Smad4 knockdown using siRNA duplex oligo ribonucleotides

TSP-1 or *DPC4* suppression was induced with small interfering RNA (siRNA) and stealth RNAi siRNA duplex oligo nucleotides (Invitrogen). Cells were plated in 6-well culture plates and duplex siRNA was transfected using Lipofectamine 3000 Transfection Reagent (Invitrogen) according to the manufacturer's instructions. Whole cell lysates were generated 48 h after transfection. Three different siRNAs were designed and purchased for each target gene (stealth RNAi siRNA; Invitrogen), and the two effective siRNAs were used in subsequent experiments. The most effective sequences were, si*TSP-1*, 5′-CCAGAUCAGGCAGACACAGACAACA-3′ and si*DPC4*, 5′-GCCCUAUUGUUACUGUUGA-3′, and the complementary sequences of each oligo. The negative control siRNA was stealth RNAi Negative Control Duplexes (Medium GC Duplex) (Invitrogen).

Expression vectors

cDNA corresponding to human *THBS1* was introduced into pLenti-C-Myc-DDK-IRES-Puro Lentiviral Gene Expression Vector (#PS100069; Origene) as previously described [28]. Human *TSP-1* cDNA was amplified with a forward primer (5'-ATGGGGCTGGCCTGGGGACTA-3') and a reverse primer (5'-TTAGGGATCTCTACATTCGTATTTCAGGTCAGAG-3') using cDNA from isolated from SK-Hep-1 cells as a template, and the product was ligated into Target Clone -Plus- (Toyobo). The full sequence of *TSP-1* cDNA was validated by Sanger sequencing. The ORF of *TSP-1* was cloned into the destination vector pLenti-C-Myc-DDK-IRES-Puro Tagged Cloning Vector (#PS100069; Origene) using In-Fusion Snap Assembly Master Mix (#638947; TaKaRa). Transformation was performed in NEB Stable Competent E. coli (#C3040I; New England BioLabs) according to the manufacturer's instructions. The final vector sequences were validated by Sanger sequencing. Lentivirus particles were produced using the Lentiviral High Titer Packaging Mix (#6194; TaKaRa) according to the manufacturer's instructions. Briefly, the destination vectors and Lentiviral High Titer Packaging Mix were transfected into cells from the Lenti-X 293T Cell Line (#Z2180N; TaKaRa) using Lipofectamine 3000 (Thermo Fisher Scientific). After a 48-h incubation, the media containing lentivirus particles was collected and passed through a 0.45-mm filter. To establish TSP-1-overexpressing PDAC cells, PDACs were cultured in medium containing virus particles with 8 ug/ml polybrene for 24 h.

Animal studies

All animal studies were conducted according to the guidelines of the Animal Care and Use Committee of Kumamoto University (approval number A2021-130). Six-week-old male BALB/c nude mice (Clea Japan, Shizuoka, Japan) were subcutaneously inoculated in both flanks with empty vector or TSP-1-overexpressing stable transfectant AsPC-1 cells (1×10^6 per mouse). The tumor size was measured twice weekly using a digital caliper (VWR International, GA) and the tumor volume was determined with the formula: tumor volume [mm^3] = (length [mm]) × (width [mm])^2 × 0.52. Twenty-one days from the start of injections mice were killed and tumors were excised, measured, and weighed.

Statistical analysis

All the experiments were performed in triplicate, and the data shown are representative of consistent results. Data are presented as the mean ± standard deviation (SD). The Mann-Whitney U test was used to compare continuous variables between 2 groups. Kaplan–Meier curves and the generalized Wilcoxon test were used to evaluate the statistical significance of the differences. Data analysis was performed with JMP (version 9, SAS Institute, Japan). A *P*-value of 0.05 was considered significant and n are reported in the figure legends.

Results

High substrate stiffness stimulates TSP-1 expression in CAFs and knockdown of TSP-1 inhibited cell proliferation with suppressed profibrogenic and activated stroma-related gene expression

PDAC is characterized by abundant stroma. We examined whether stiffness stimulates TSP-1 expression in CAFs. Culture of CAFs on high substrate stiffness (16 kPa) induced morphological changes to a spindle shape compared with those on low substrate stiffness (0.2 kPa) (Fig. 1A). On high substrate stiffness, TSP-1 was strongly expressed around the nuclei of enlarged CAFs, as detected by immunofluorescence staining (Fig. 1B, C). Culture on high substrate stiffness enhanced the expression of TSP-1, connective tissue growth factor (CTGF), and Fibronectin, and further stimulated phosphorylation of Akt compared with low stiffness in CAFs (Figs. 1D, E and S1A). These results indicated that high stiffness substrate stimulated TSP-1 expression with a profibrogenic phenotype in CAFs.

To investigate the biological role of TSP-1 in CAFs, knockdown of *TSP-1* was performed using siRNA (Figs. 1F and S1B). Knockdown of *TSP-1* attenuated cell proliferation compared with the control in CAFs (Fig. 1G) and suppressed CTGF expression and phosphorylation of Akt (Figs. 1H and S1C). Recent comprehensive genomic studies have elucidated the subtypes of PDAC, which link malignant behavior and prognostic outcomes based on molecular information [29–32]. Especially,

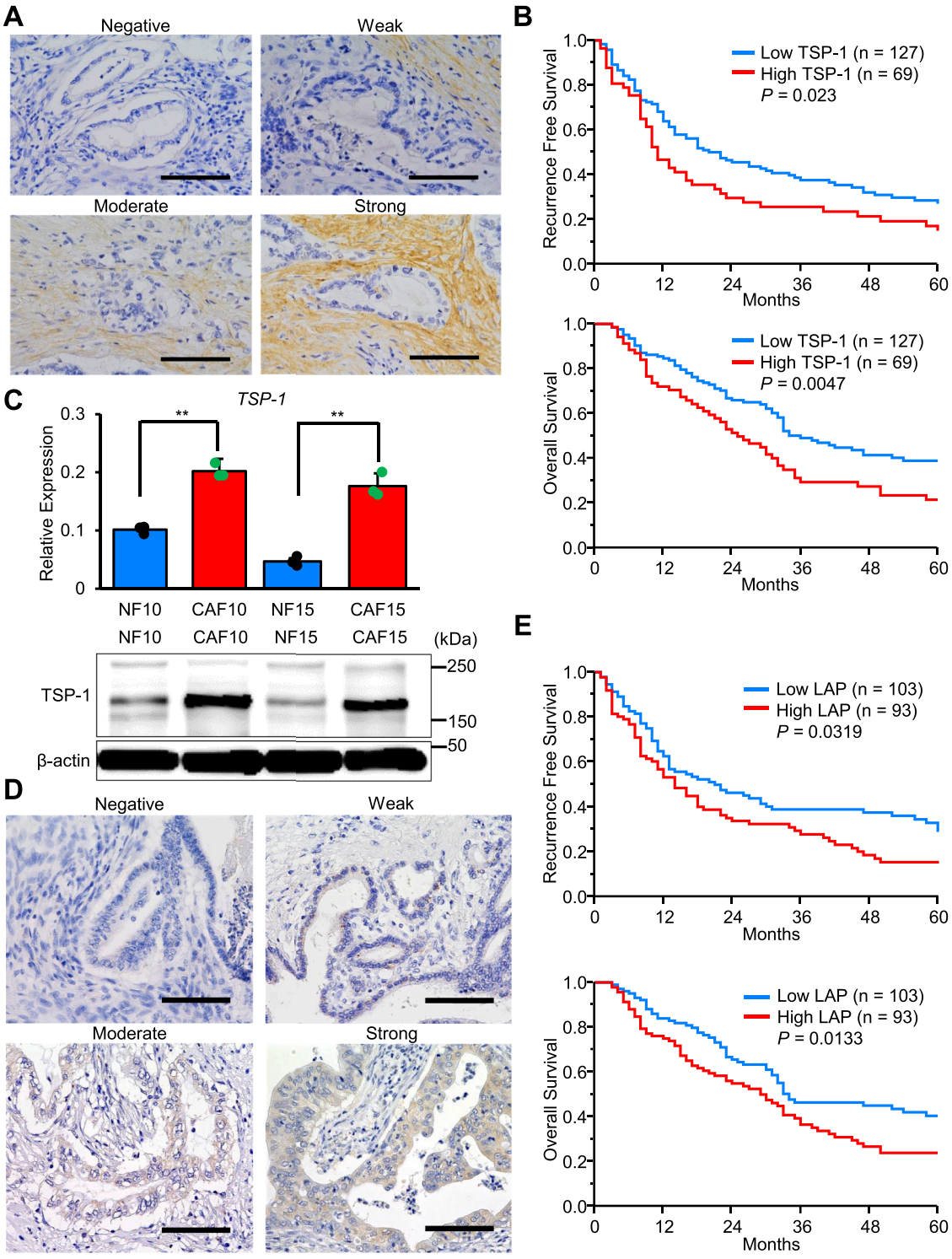

Fig. 2. *Overexpression of TSP-1 in stroma and LAP in cancer cells were associated with worse prognostic outcomes in PDAC patients.* A Immunohistochemical analysis of TSP-1 protein expression in human PDAC tissue ($n = 196$). TSP-1 is predominantly expressed in cancer stroma. The figure illustrates examples with negative, weak (upper panels) and moderate, strong (lower panels) staining intensity. Representative images are shown. Scale bars, 100 μm. B Kaplan–Meier curves of RFS (upper panel) and OS (lower panel) according to TSP-1 expression levels in cancer stroma. C TSP-1 expression levels in NFs and CAFs. Upper panel) *TSP-1* mRNA expression levels were examined by qRT-PCR. Data were normalized to the amount of *β-actin* mRNA serving as the internal control. Lower panel) TSP-1 protein expression was examined by western blot analysis. β-actin served as a loading control. Representative blots are shown (**$P < 0.01$; $n = 3$). D Immunohistochemical analysis of LAP in human PDAC tissue ($n = 196$). LAP is expressed in the nucleus and/or cytoplasm in PDAC tissues. The figure illustrates examples with negative, weak (upper panels) and moderate, strong (lower panels) staining intensity. Representative images are shown. Scale bars, 100 mm. E Kaplan–Meier curves of RFS (upper panel) and OS (lower panel) according to LAP expression levels in the nucleus and/or cytoplasm.

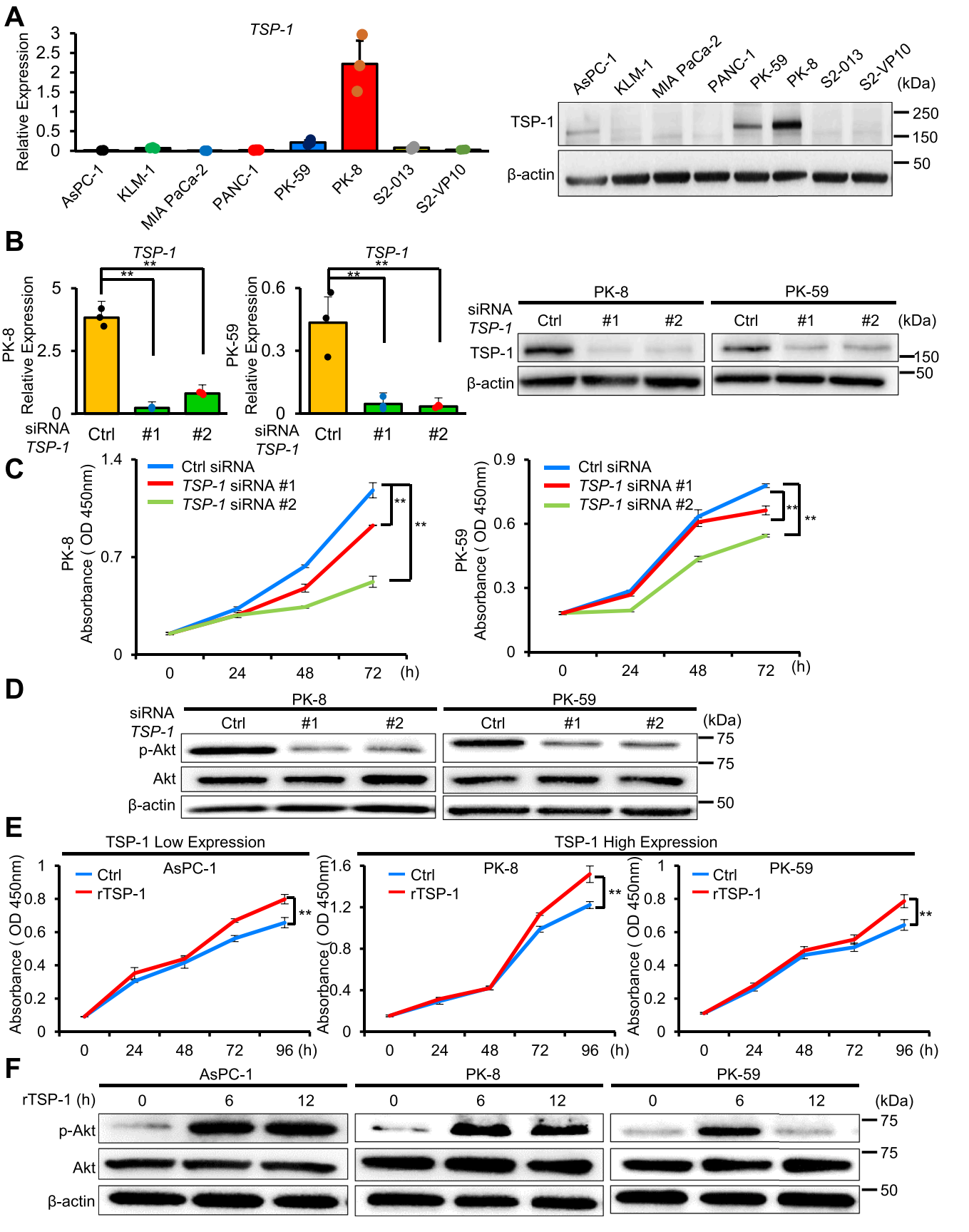

(caption on next page)

Fig. 3. *TSP-1 promotes cell proliferation via Akt signal activation in a paracrine and autocrine manner in PDAC cells.* A TSP-1 expression in 8 PDAC cell lines. Left panel) qRT-PCR analysis of *TSP-1* mRNA was performed. The results were normalized to the *β-actin* loading control. Right panel) Western blot analysis of TSP-1 protein was performed. β-actin protein expression served as a loading control. Representative blots are shown ($n = 3$). B Knockdown of *TSP-1* was performed using siRNA in TSP-1-positive cells (PK-8 and PK-59). qRT-PCR and western blot analyses were performed 48 h after *TSP-1* knockdown (**$P < 0.01$; $n = 3$). C Cell proliferation assay in PDAC cells with *TSP-1* knockdown (**$P < 0.01$; $n = 3$). D Knockdown of *TSP-1* in PDAC cells (PK-8 and PK-59) suppressed phosphorylation of Akt at 48 h, as detected by western blot analysis. β-actin was used as a loading control. Representative blots are shown ($n = 3$). E Cell proliferation assay under treatment with rTSP-1 (1 μg/ml) was performed using TSP-1-negative (AsPC-1) and -positive (PK-8 and PK-59) cell lines (**$P < 0.01$; $n = 3$). F The phosphorylation of Akt in TSP-1-negative (AsPC-1) and -positive (PK-8 and PK-59) cell lines treated with rTSP-1 (1 μg/ml) was evaluated by western blot at the indicated times. β-actin was used as a loading control. Representative blots are shown ($n = 3$).

Moffitt et al. [31] categorized PDAC tumors into two subtypes according to genetic expression patterns in tumor stroma. The activated stromal subtype with *ITGAM* and *FAP* expression showed a worse prognosis compared with the normal stromal subtype [31]. In this study, knockdown of *TSP-1* attenuated the expression of activated stroma-related genes (*ITGAM* and *FAP*) compared with the controls (Fig. 1I). These findings indicated that TSP-1 played a crucial role in the proliferative activity and profibrotic response of CAFs, revealing an activated stroma subtype in PDAC.

Overexpression of TSP-1 in stroma and LAP in cancer cells were associated with worse prognostic outcomes in PDAC patients

We examined the expression patterns of TSP-1 and LAP, the latent form of TGF-β, in PDAC human tissues. TSP-1 expression was detected in 161 (82.1%) of 196 cases by immunohistochemistry (IHC) staining and was predominantly expressed in cancer stromal tissue. In limited cases ($n = 17$, 8.7%) among 196 cases, cancer cells were also positive for TSP-1 by IHC staining (Fig. S2). These findings indicated that TSP-1 was predominantly produced by cancer stroma cells rather than cancer cells in PDAC. According to the intensity of TSP-1 staining in the stroma, 35 patients (17.9%) were categorized as "negative", 92 patients (46.9%) as "weak", 63 patients (32.1%) as "moderate", and 6 patients (3.1%) as "strong" (Fig. 2A). Patients with low scores were classified as "low expression" ($n = 127$; 64.8%), whereas patients with high scores were defined as "high expression" ($n = 69$; 35.2%). We subsequently assessed the clinical impact of TSP-1 expression levels in cancer stroma on the prognostic outcome of PDAC patients with pancreatic resection. High TSP-1 expression was significantly associated with worse prognostic outcomes in RFS and OS compared with those with low TSP-1 expression ($P = 0.023$ and $P = 0.0047$, respectively) (Fig. 2B). The median survival time in the high and low stromal TSP-1 expression groups was 26.2 and 35.1 months, respectively. Using established CAFs and NFs from resected human PDAC tissues, we further confirmed that CAFs stimulated higher TSP-1 expression compared with NFs (Figs. 2C and S1D). TSP-1 is a major activator of TGF-β1 in vivo [22]. Next, the expression of LAP was examined in human PDAC tissues by IHC staining. LAP expression was detected in the nuclei and/or cytoplasm of cancer cells 180 patients (91.8%) (Fig. 2D) and stromal cells also expressed LAP in 36 patients (18.4%). Cancer cells were excessively positive for LAP compared with stroma cells. These findings suggested that LAP was predominantly expressed by cancer cells in PDAC tissue. According to the intensity of LAP staining in cancer cells, 16 patients (8.2%) were classified as "negative", 87 patients (44.4%) as "weak", 75 patients (38.3%) as "moderate", and 18 patients (9.1%) as "strong". Furthermore, high LAP expression ($n = 93$) in cancer cells was significantly associated with worse prognostic outcomes in RFS and OS compared with those with low LAP expression ($n = 103$) ($P = 0.0319$ and $P = 0.0133$, respectively) (Fig. 2E). The median survival time in patients with high and low LAP expression levels was 29.6 and 34.4 months, respectively. These results suggested that TSP-1 derived from CAFs and local TGF-β signal activation in cancer cells was associated with malignant behavior in PDAC.

TSP-1 plays a crucial role in cell proliferation and EMT in a paracrine and autocrine manner in PDAC cells

The biological roles of TSP-1 in PDAC cells were examined. Although TSP-1 was predominantly expressed in the stromal tissue of human PDAC, cancer cells also expressed TSP-1 in some cases, as mentioned above. Among 8 human PDAC cell lines, strong TSP-1 expression was detected in PK-8 and PK-59 (Fig. 3A). In these two TSP-1-positive cell lines, knockdown of *TSP-1* was performed to investigate the biological role of TSP-1 in cancer cells (Figs. 3B and S1E). Knockdown of *TSP-1* in PDAC cancer cells attenuated cell proliferation and phosphorylation of Akt (Figs. 3C, D and S1F). Next, we examined the paracrine effect of TSP-1 in PDAC cancer cells because TSP-1 was predominantly expressed by CAFs in human PDAC tissues. Interestingly, treatment with rTSP-1 promoted cell proliferation and phosphorylation of Akt both in TSP-1-negative (AsPC-1) and -positive (PK-8 and PK-59) PDAC cell lines (Figs. 3E, F and S1G). These results indicated that TSP-1 accelerated cell proliferation rate with activated Akt signal in a paracrine and autocrine manner in PDAC cells.

In addition, we examined the biological effect of TSP-1 on EMT in PDAC cells because TSP-1 is a major activator of TGF-β1, which is a potent inducer of EMT. Treatment with the rTSP-1 promoted cancer invasion (Fig. 4A). In addition, treatment of TSP-1-negative (AsPC-1) and -positive (PK-8 and PK-59) PDAC cell lines with rTSP-1 promoted the phosphorylation of Smad2/3 with altered expression of EMT markers (loss of E-cadherin and gain of N-cadherin) (Figs. 4B and S1H). In contrast, knockdown of *TSP-1* in TSP-1-positive cells (PK-8 and PK-59) attenuated cell invasiveness and phosphorylation of Smad2/3 with the altered expression of EMT markers (gain of E-cadherin and loss of N-cadherin) (Figs. 4C, D and S1I). These findings indicated that TSP-1 functioned as an EMT inducer via TGF-β/Smad signal activation in a paracrine and autocrine manner in PDAC cells.

Downregulation of Smad4 expression induces TSP-1 overexpression with TGF-β signal activation in PDAC

In the multistep process of PDAC carcinogenesis, loss of Smad4 triggers accelerated cell invasiveness and metastatic potential with TGF-β signal activation [29]. Smad4 expression in cancer cells was undetectable in 82 (42%) of 196 cases by IHC staining (Fig. 5A). Smad4-negative expression was significantly associated with worse prognostic outcomes in RFS and OS compared with those with Smad4-positive expression ($P < 0.0001$ for both) (Fig. 5B). Among 8 human PDAC cell lines, strong Smad4 expression was detected in AsPC-1, MIA PaCa-2, PANC-1, and PK-59 (Fig. 5C). Surprisingly, knockdown of *DPC4* induced TSP-1 overexpression with accelerated phosphorylation of Smad2/3 and Akt expression in Smad4-positive cells (PK-59 and MIA PaCa-2) (Figs. 5D and S1J). We further analyzed the clinical impact of Smad4 and TSP-1 expression on the prognostic outcomes of PDAC patients. Double-positivity was detected in 16.8% of patients, while Smad4 or TSP-1 single-positivity was identified in 41.8% and 18.3% patients, respectively. Double-negativity was found in 23.1% of patients. Among them, Smad4-negativity/TSP-1-positivity was associated with worst prognostic outcomes of RFS and OS in patients with pancreatic resection for PDAC, whereas Smad4-positivity/TSP-1-negativity revealed the most favorable prognostic outcomes (Fig. 5E).

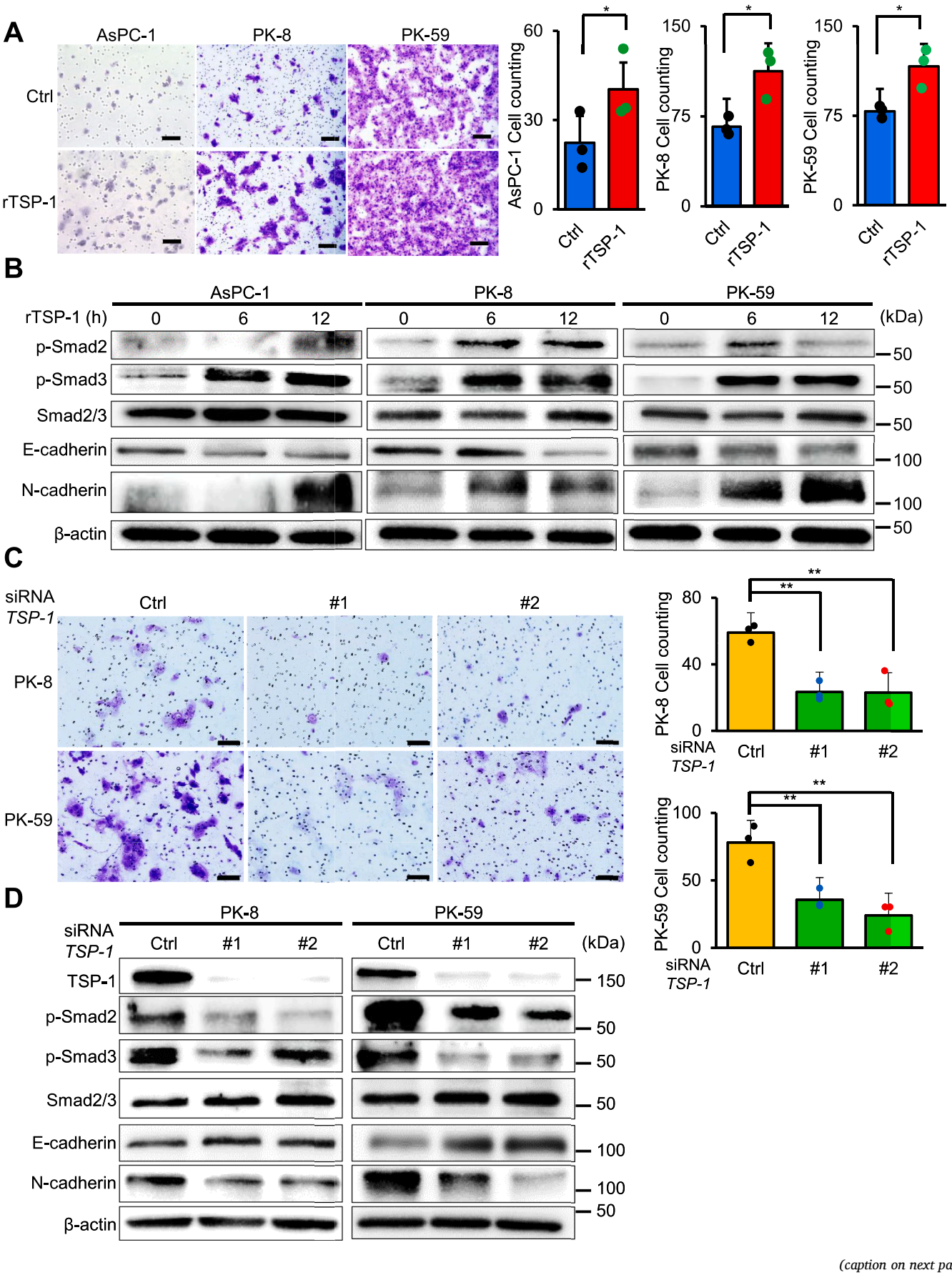

(caption on next page)

Fig. 4. *TSP-1 promotes EMT via TGF-β/Smad signal activation in a paracrine and autocrine manner in PDAC cells.* A Cell invasion assay was performed under treatment with rTSP-1 (1 μg/ml) in AsPC-1, PK-8, and PK-59 cells. Representative images are shown in the left panels, and three randomly selected fields are quantified on the right panels (*$P < 0.05$; $n = 3$). Scale bars, 100 mm. B Western blot analysis of Smad2/3 and EMT markers (E-cadherin and N-cadherin) in TSP-1-negative (AsPC-1) and -positive (PK-8 and PK-59) cell lines treated with rTSP-1 (1 μg/ml) for the indicated time. β-actin protein expression served as a loading control. Representative blots are shown ($n = 3$). C Cell invasion assay in PDAC cells (PK-8 and PK-59) with *TSP-1* knockdown was performed. Representative images are shown in the left panels, and three randomly selected fields are quantified in the right panels (**$P < 0.01$; $n = 3$). Scale bars, 100 mm. D Western blot analysis of Smad2/3 and EMT markers (E-cadherin and N-cadherin) in PDAC cells (PK-8 and PK-59) with *TSP-1* knockdown. β-actin protein expression served as a loading control. Representative blots are shown ($n = 3$).

The median survival times in patients with Smad4-negativity/TSP-1-positivity and Smad4-positivity/TSP-1-negativity expression were 19.5 and 52.4 months, respectively. These findings suggest that downregulation of Smad4 expression and TSP-1 overexpression were associated with worse prognostic outcomes in PDAC and that downregulation of Smad4 expression triggered TSP-1 expression with TGF-β signal activation and promoted malignant behavior in PDAC.

TSP-1 overexpression induces downregulation of Smad4 expression and enhances cell proliferation in vitro and in vivo

The biological effects of TSP-1 expression in cancer cells were examined. Stable TSP-1-overexpressing cells were established using AsPC-1 cells with low TSP-1 expression (Fig. 6A). Interestingly, overexpression of TSP-1 in AsPC-1 cells induced downregulation of Smad4 expression and enhanced phosphorylation of Akt (Figs. 6B and S1K). Furthermore, overexpression of TSP-1 in AsPC-1 cells promoted cell proliferation compared with the controls (Fig. 6C). Thus, TSP-1 and Smad4 exhibited a mutual double negative feedback loop (Fig. 6D). In an in vivo experiment using a xenograft model, tumors with TSP-1 expression displayed enhanced tumor volumes after 21 days compared with the controls (Fig. 6E–G). Furthermore, tumors with TSP-1 expression had more cancer cells with mesenchymal features (loss of E-cadherin and gain of Vimentin) invading into the surrounding tissue at the invasive front compared with the controls (Fig. 6H).

LSKL peptide, which inhibits TSP-1 binding to LAP and the subsequent TGF-β signal activation, displays anti-cancer effects in PDAC cells

To examine the therapeutic potential of inhibiting TSP-1-mediated TGF-β signal activation, PK-8 cells were treated with LSKL peptide, which inhibits TSP-1 binding to LAP and the subsequent TGF-β signal activation. LSKL peptide treatment inhibited cell proliferation and migration compared with SLLK peptide treatment (control peptide) (Fig. 7A, B). Furthermore, treatment with LSKL peptide in PK-8 cells suppressed phosphorylation of Akt (Figs. 7C and S1L). Next, we examined whether LSKL peptide could overcome chemoresistance for L-OHP in PK-8 cells. PK-8 cells were treated with different concentrations of L-OHP (0.001–100 μM) and cell viability was determined by Cell proliferation assay (Fig. S3). LSKL peptide treatment with L-OHP enhanced cell apoptosis in a cell proliferation assay, as represented by upregulated Cleaved caspase-3 expression (Figs. 7D, E and S1M). Thus, TSP-1 played a critical role in the chemoresistance. Collectively, these results suggested that LSKL peptide could be a novel therapeutic approach in PDAC by antagonizing TSP-1-mediated latent TGF-β activation.

Discussion

Here, we identified a novel biological role of TSP-1 in PDAC progression (Fig. 7F). PDAC is characterized by abundant stroma. In this study, high substrate stiffness promoted TSP-1 expression in CAFs. For CAFs themselves, TSP-1 played a crucial role in the proliferative activity and profibrotic response with activated stroma subtype in PDAC. TSP-1 inhibition suppressed the expression of activated stroma subtype-related genes, suggesting that TSP-1 could be a therapeutic target in the tumor microenvironment of PDAC. Furthermore, TSP-1 overexpression in CAFs and LAP overexpression in cancer cells were worse prognostic factors in patients with surgically resected PDAC, suggesting that TSP-1 derived from cancer stroma and local TGF-β signal activation in cancer cells play a crucial role in acquired malignant behavior in PDAC microenvironment. In the current study with a relative larger number of PDAC cases, TSP-1 expression patterns were similar to two previous reports [33,34] and the high TSP-1 expression in desmoplastic stroma was further identified as a worse prognostic marker in patients with surgically resected PDAC. Furthermore, we examined LAP expression patterns in PDAC tissues. In 93 cases (47.4%), cancer epithelial cells showed moderate and strong positivity for LAP. Additionally, high LAP expression was identified as a worse prognostic marker in patients with surgically resected PDAC. LAP is required for the correct folding of the TGF-β homodimer and its secretion from cells. Furthermore, LAP shields the receptor binding epitope of mature TGF-β, indicating that LAP renders TGF-β biologically inactive and prevents interactions of TGF-β with receptors [21]. When TSP-1 binds to the LAP/TGF-β complex, TGF-β is released from LAP or latent TGF-β complex undergoes conformational change [21,35]. Therefore, active TGF-β is exposed to the TGF-β receptor binding site, and TGF-β signals through Smad phosphorylation. Furthermore, knockdown and overexpression of TSP-1 do not affect the expression of TGF-β1 itself in pancreatic cancer cells (Fig. S4). These findings suggest that stroma-derived TSP-1 interacts with LAP in cancer cells and then activates local TGF-β signal during PDAC progression.

Although TSP-1 expression in PDAC was almost all localized to desmoplastic stroma, elective cancer cells of PDAC tissues and PDAC cell lines were also positive for TSP-1 expression in this study. In PDAC cells, TSP-1 acted as an EMT inducer via TGF-β/Smad signal activation and promoted malignant behavior in a paracrine and autocrine manner in PDAC cells. SB431542, inhibitor of the kinase function of the TGF-β type I receptor, reduced Smad2/3 phosphorylation and blocked the TGF-β-mediated EMT (Fig. S5). Furthermore, downregulation of Smad4 expression triggered TSP-1 overexpression with TGF-β signal activation in cancer cells and promoted malignant behavior in PDAC. Oshima et al. [12] previously reported that downregulation of Smad4 immunolabeling was an independent poor prognostic factor in 106 resectable PDAC. During PDAC carcinogenesis, downregulation of Smad4 is an important step in acquiring malignant behavior such as high invasiveness and metastatic potential [29,36,37]. The high invasiveness and metastatic potential are not increased directly by the downregulation of Smad4, but these are regulated in cooperation with other genes [38]. Intriguing, this study elucidated that TSP-1 overexpression also induced downregulation of Smad4 expression in PDAC cells. Furthermore, TGF-β treatment also enhances the TSP-1 expression, and results in decreased Smad4 expression in PDAC cells (Fig. S6). Downregulation Smad4 caused upregulation of cell cycle-related genes (Fig. S7) [39]. This study is the first to report the interplay between downregulation of Smad4 and TGF-β signal activation via TSP-1 during PDAC progression.

Clinical trials of a therapeutic strategy targeting TSP-1 except LSKL peptide have been conducted in colorectal cancer and renal cell carcinoma but not PDAC [40,41]. However, these two trials failed to show an improvement in prognosis and resulted in severe adverse effects [40,41]. In the current study, LSKL peptide treatment attenuated Akt signal activation, and the combined administration of LSKL peptide and chemotherapy (L-OHP) enhanced apoptosis in PDAC cells. The anti-tumor effect of LSKL peptide has also been demonstrated in thyroid carcinoma and multiple myeloma, and the effect was impressive in combination with chemotherapy rather than a single agent, although the

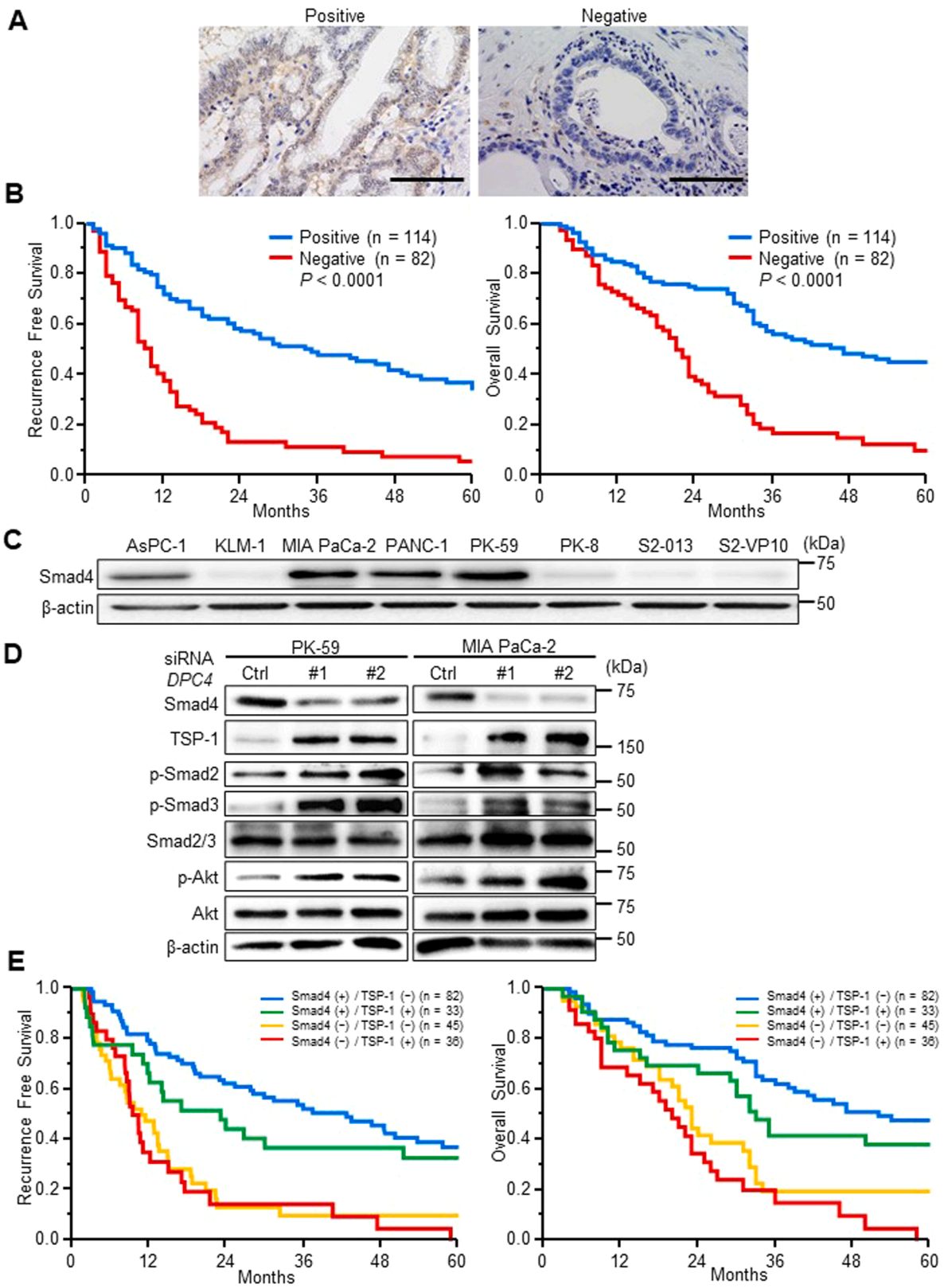

Fig. 5. *Downregulation of Smad4 expression triggered TSP-1 overexpression with TGF-β signal activation and was associated with worse prognostic outcomes in PDAC.* A Immunohistochemical analysis of Smad4 expression in 196 PDAC tissue samples. Smad4 protein expression was localized to the nuclei and/or cytoplasm of cancer cells. Representative images are shown. Scale bars, 100 μm. B Kaplan–Meier curves for RFS (left panel) and OS (right panel) according to Smad4 expression. C Western blot analysis of Smad4 expression in 8 PDAC cell lines. β-actin protein expression served as a loading control. Representative blots are shown ($n = 3$). D Western blot analysis of TSP-1, phosphorylated Smad2/3, and phosphorylated Akt in PDAC cells (PK-59 and MIA PaCa-2) with *DPC4* knockdown. β-actin protein expression served as a loading control. Representative blots are shown ($n = 3$). E Kaplan–Meier curves for RFS (left panel) and OS (right panel) according to Smad4 and TSP-1 expression.

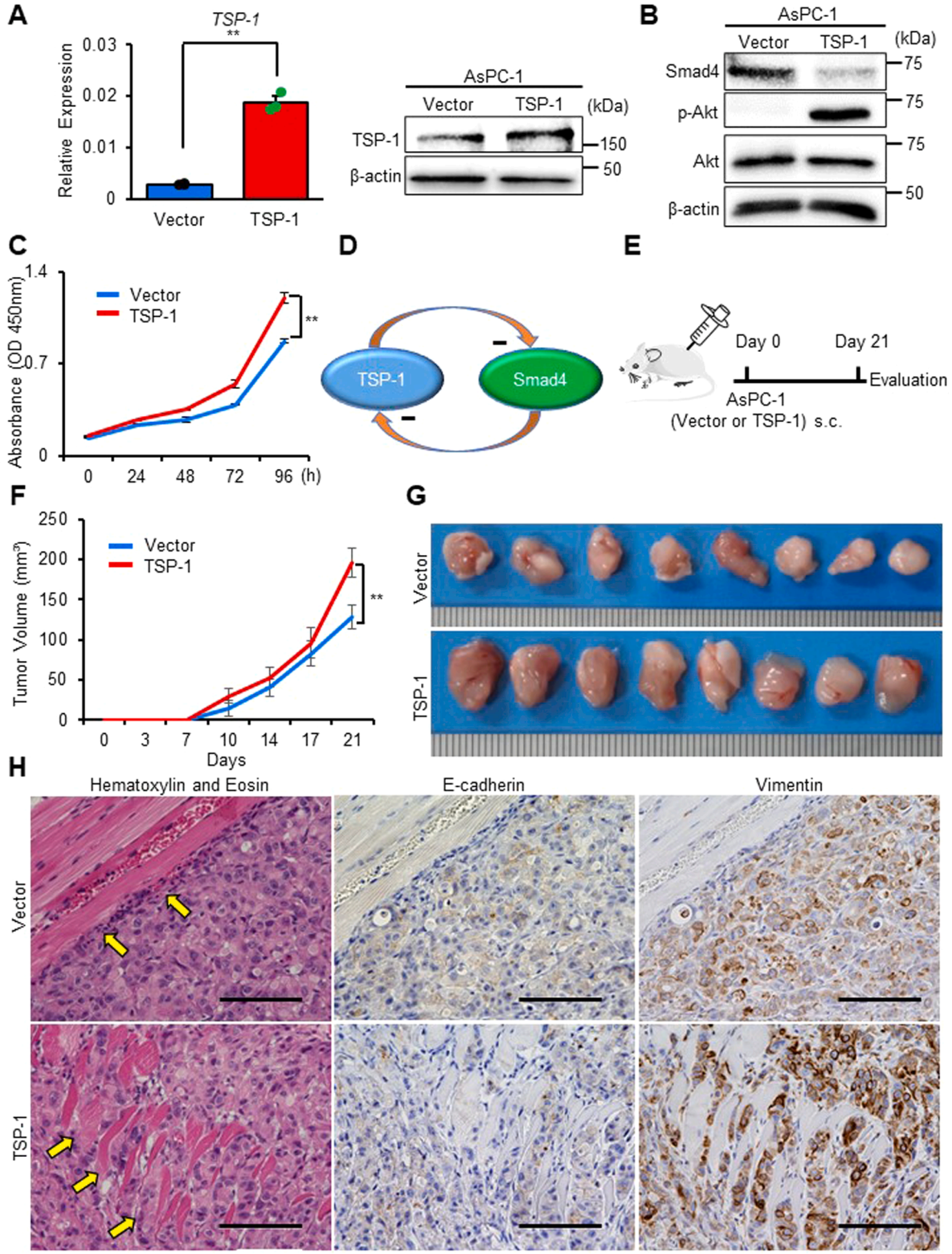

Fig. 6. *TSP-1 expression induced downregulation of Smad4 expression and enhanced cell proliferation and invasiveness in vitro and in vivo.* A Stable TSP-1-overexpressing cells were established using AsPC-1 cell lines. TSP-1 expression at the mRNA and protein level was confirmed by qRT-PCR (left panel) and western blot (right panel) (**$P < 0.01$; $n = 3$). B Western blot analysis of Smad4 and phosphorylation of Akt. β-actin protein expression served as a loading control. Representative blots are shown ($n = 3$). C Cell proliferation assays in AsPC-1 cells with TSP-1 overexpression (**$P < 0.01$; $n = 3$). D Schema of a supposed mutual double negative feedback loop. E Schema of the experimental procedure ($n = 8$ in each group). AsPC-1 cells with TSP-1 overexpression or control were injected subcutaneously in nude mice. Mice were killed at 21 days. F Tumor volume was measured twice weekly for 21 days (**$P < 0.01$; $n = 8$). Tumor volume was calculated using the formula: tumor volume [mm^3] = (length [mm]) × (width [mm])^2 × 0.52. G Gross morphologies of extracted tumors at 21 days are shown ($n = 8$). H Microscopic findings (hematoxylin-eosin, E-cadherin, and Vimentin staining) at the invasive front in extracted tumors with control vector and TSP-1 overexpression. Scale bars, 100 μm.

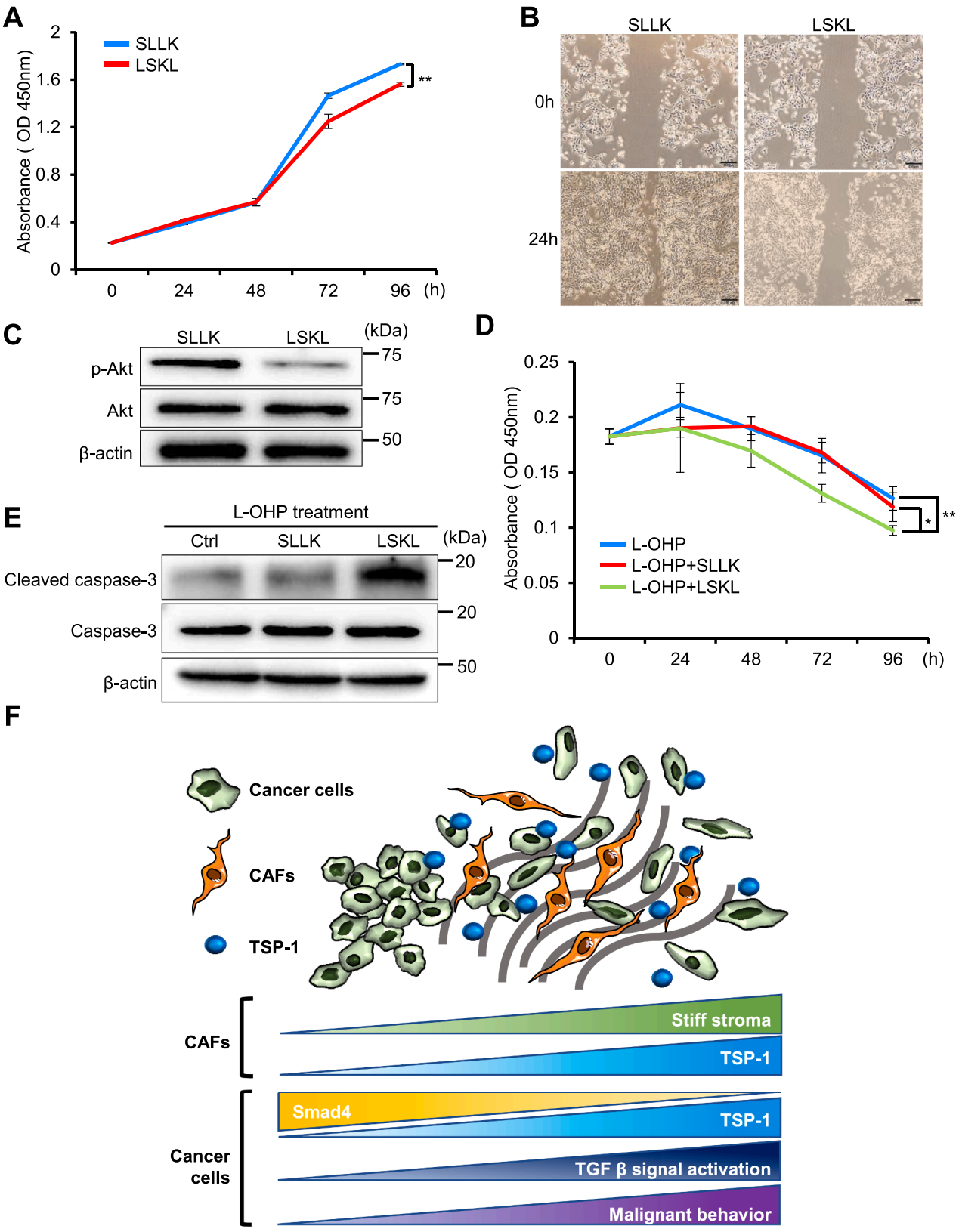

Fig. 7. *Therapeutic potential of LSKL peptide by antagonizing TSP-1-mediated latent TGF-β activation in PDAC cells.* A Cell proliferation assay was performed in PK-8 cells treated with LSKL peptide or control (SLLK peptide) (**$P < 0.01$; $n = 3$). B Wound healing assay was performed in PK-8 cells treated with LSKL peptide or control (SLLK peptide). Representative phase-contrast microscope images at 0 h and 24 h are shown ($n = 3$). C Western blot analysis of Akt phosphorylation in PK-8 cells at 12 h after LSKL peptide or control (SLLK peptide) treatment. β-actin protein expression served as a loading control. Representative blots are shown ($n = 3$). D Proliferation assay for L-OHP was performed in PK-8 cells treated with LSKL peptide or control (SLLK peptide) (*$P < 0.5$ and ** $P < 0.01$; $n = 3$). E Western blot analysis of Cleaved caspase-3 in PK-8 cells at 12 h after L-OHP and LSKL peptide or control (SLLK peptide) treatment. β-actin protein expression served as a loading control. Representative blots are shown. F Schema of the biological roles of TSP-1 in PDAC progression.

reasons for this observation was not elucidated in these studies [42,43]. Further clinical trials using LSKL peptide with anti-cancer agents may be required for patients with PDAC.

There are several limitations to this study. Integrin avb6 is another major activator of local TGF-β signal in vivo [44], and the local TGF-β signal activation mechanism is likely to be tissue-specific [45]. In this study, the expression and biological role of integrin avb6 was not investigated. Another limitation is that it is unclear which of Smad4 downregulation and TSP-1 overexpression plays an important role as an initial step in cancer cells during PDAC carcinogenesis. TSP-1 derived from CAFs may promote downregulation of Smad4 in cancer cells in the tumor microenvironment. Interestingly, PK-59 cells have robust Smad4 expression and relative high TSP-1 expression. In human resected samples, approximately 17% of tumors reveals high TSP-1 expression in stroma cells and Smad4 expression in cancer cells by IHC staining. There findings suggest an alternative mechanism of interplay between TSP-1 and Smad4 during PDAC progression. In the clinical setting, no established therapeutic strategies using TSP-1 inhibitor for cancer treatment are currently available [46]. We hope to initiate clinical trials to elucidate the potential of TSP-1 inhibitor or LSKL peptide as a therapeutic approach for PDAC patients worldwide.

In summary, TSP-1 derived from CAFs stimulates downregulation of Smad4 expression in cancer cells and accelerates malignant behavior by TGF-β signal activation in PDAC. TSP-1 could be a novel therapeutic target, not only for CAFs in stiff stroma, but also for cancer cells in the PDAC microenvironment.

Authors' contributions

Conceived and designed the experiments: KM and HH. Performed the experiments: NY, TH, KS, YF. Analyzed the data: HH, NY. Wrote the manuscript: HH, KM. Collected clinical samples: KH, SN, KM, HN, DH, AC. Provided critical revisions for scientific findings: TI, TB. Organized the paper and approved the final version to be published: HH and HB.

Funding

This work was supported by a Grant-in-Aid for Scientists (C); the Ministry of Education, Culture, Sports, Science, and Technology of Japan, No. 19K09177 (to H.H.); and the Takeda Science Foundation, Japan (to H.H.).

Availability of data and materials

All data generated or analyzed during this study are included in this published article and its additional files.

Ethics approval and consent to participate

The study was approved by the medical ethics committee of Kumamoto University (project no. 1291), and written informed consent was obtained from the human subjects. All animal studies were conducted according to the guidelines of the Animal Care and Use Committee of Kumamoto University (Approval No. A2021-130).

Consent for publication

All authors have agreed to publish this manuscript.

Declaration of Competing Interest

No conflicts of interest, financial or otherwise, have been declared by the authors.

Acknowledgments

The authors thank Dr. Hiromitsu Hayashi and Dr. Norio Uemura for helping with the study; Ms. Yasuda and Ms. Ogata for their excellent technical assistance; Dr. Fumimasa Kitamura for giving me good advices; Dr. Takayoshi Kaida, Takaaki Higashi, Shigeki Nakagawa, Kosuke Mima, Katsunori Imai, Yo-ichi Yamashita and Prof. Hideo Baba for assistance with revision of the paper. We thank H. Nikki March, PhD, from Edanz (https://jp.edanz.com/ac) for editing a draft of this manuscript.

Supplementary materials

Supplementary material associated with this article can be found, in the online version, at doi:10.1016/j.tranon.2022.101533.

References

[1] R.L. Siegel, K.D. Miller, A. Jemal, Cancer statistics, 2019, CA Cancer J. Clin. 69 (2019) 7–34.
[2] D. von Ahrens, T.D. Bhagat, D. Nagrath, A. Maitra, A. Verma, The role of stromal cancer-associated fibroblasts in pancreatic cancer, J. Hematol. Oncol. 10 (2017) 76.
[3] B.M. MacCurtain, N.P. Quirke, S.D. Thorpe, T.K. Gallagher, Pancreatic ductal adenocarcinoma: relating biomechanics and prognosis, J. Clin. Med. 10 (2021).
[4] J. Winkler, A. Abisoye-Ogunniyan, K.J. Metcalf, Z. Werb, Concepts of extracellular matrix remodelling in tumour progression and metastasis, Nat. Commun. 11 (2020) 5120.
[5] M.A. Nieto, Y.J. Huang Ruby, A. Jackson Rebecca, P. Thiery Jean, EMT: 2016, Cell 166 (2016) 21–45.
[6] L. Peng, D. Wang, Y. Han, T. Huang, X. He, J. Wang, et al., Emerging role of cancer-associated fibroblasts-derived exosomes in tumorigenesis, Front. Immunol. 12 (2021), 795372.
[7] A. Moustakas, C.H. Heldin, Mechanisms of TGFβ-induced epithelial–mesenchymal transition, J. Clin. Med. 5 (2016) 63.
[8] S. Ahmed, A.D. Bradshaw, S. Gera, M.Z. Dewan, R. Xu, The TGF-β/Smad4 signaling pathway in pancreatic carcinogenesis and its clinical significance, J. Clin. Med. 6 (2017).
[9] M. Zhao, L. Mishra, C.X. Deng, The role of TGF-beta/Smad4 signaling in cancer, Int. J. Biol. Sci. 14 (2018) 111–123.
[10] S. Yachida, C.M. White, Y. Naito, Y. Zhong, J.A. Brosnan, A.M. Macgregor-Das, et al., Clinical significance of the genetic landscape of pancreatic cancer and implications for identification of potential long-term survivors, Clin. Cancer Res. 18 (2012) 6339–6347.
[11] H. Hayashi, T. Kohno, H. Ueno, N. Hiraoka, S. Kondo, M. Saito, et al., Utility of assessing the number of mutated KRAS, CDKN2A, TP53, and Smad4 genes using a targeted deep sequencing assay as a prognostic biomarker for pancreatic cancer, Pancreas 46 (2017) 335–340.
[12] M. Oshima, K. Okano, S. Muraki, R. Haba, T. Maeba, Y. Suzuki, et al., Immunohistochemically detected expression of 3 major genes (CDKN2A/p16, TP53, and Smad4/DPC4) strongly predicts survival in patients with resectable pancreatic cancer, Ann. Surg. 258 (2013) 336–346.
[13] J.R. Gotovac, T. Kader, J.V. Milne, K.M. Fujihara, L.E. Lara-Gonzalez, K. L. Gorringe, et al., Loss of Smad4 is sufficient to promote tumorigenesis in a model of dysplastic Barrett's esophagus, Cell. Mol. Gastroenterol. Hepatol. 12 (2021) 689–713.
[14] H. Wang, B. Stephens, D.D. Von Hoff, H. Han, Identification and characterization of a novel anticancer agent with selectivity against deleted in pancreatic cancer locus 4 (DPC4)-deficient pancreatic and colon cancer cells, Pancreas 38 (2009) 551–557.
[15] X. Xu, S. Kobayashi, W. Qiao, C. Li, C. Xiao, S. Radaeva, et al., Induction of intrahepatic cholangiocellular carcinoma by liver-specific disruption of Smad4 and Pten in mice, J. Clin. Invest. 116 (2006) 1843–1852.
[16] A.A. Aitchison, A. Veerakumarasivam, M. Vias, R. Kumar, F.C. Hamdy, D.E. Neal, et al., Promoter methylation correlates with reduced Smad4 expression in advanced prostate cancer, Prostate 68 (2008) 661–674.
[17] X. Xia, W. Wu, C. Huang, G. Cen, T. Jiang, J. Cao, et al., Smad4 and its role in pancreatic cancer, Tumour Biol. 36 (2015) 111–119.
[18] D.F. Mosher, Physiology of thrombospondin, Annu. Rev. Med. 41 (1990) 85–97.
[19] J.C. Adams, Thrombospondins: multifunctional regulators of cell interactions, Annu. Rev. Cell Dev. Biol. 17 (2001) 25–51.
[20] H. Hayashi, K. Sakai, H. Baba, T. Sakai, Thrombospondin-1 is a novel negative regulator of liver regeneration after partial hepatectomy through transforming growth factor-beta1 activation in mice, Hepatology 55 (2012) 1562–1573.
[21] H. Hayashi, T. Sakai, Biological significance of local TGF-beta activation in liver diseases, Front. Physiol. 3 (2012) 12.
[22] S.E. Crawford, V. Stellmach, J.E. Murphy-Ullrich, S.M. Ribeiro, J. Lawler, R. O. Hynes, et al., Thrombospondin-1 is a major activator of TGF-beta1 *in vivo*, Cell 93 (1998) 1159–1170.
[23] T. Yasuda, M. Koiwa, A. Yonemura, T. Akiyama, H. Baba, T. Ishimoto, Protocol to establish cancer-associated fibroblasts from surgically resected tissues and generate senescent fibroblasts, STAR Protoc. 2 (2021), 100553.

[24] K. Mima, H. Okabe, T. Ishimoto, H. Hayashi, S. Nakagawa, H. Kuroki, et al., CD44s regulates the TGF-β-mediated mesenchymal phenotype and is associated with poor prognosis in patients with hepatocellular carcinoma, Cancer Res. 72 (2012) 3414–3423.
[25] Y. Jiang, J. Xie, W. Huang, H. Chen, S. Xi, Z. Han, et al., Tumor immune microenvironment and chemosensitivity signature for predicting response to chemotherapy in gastric cancer, Cancer Immunol. Res. 7 (2019) 2065–2073.
[26] J.Z. Xu, W.Q. Wang, W.H. Zhang, H.X. Xu, H.L. Gao, S.R. Zhang, et al., The loss of Smad4/DPC4 expression associated with a strongly activated hedgehog signaling pathway predicts poor prognosis in resected pancreatic cancer, J. Cancer 10 (2019) 4123–4131.
[27] R.E. Wilentz, G.H. Su, J.L. Dai, A.B. Sparks, P. Argani, T.A. Sohn, et al., Immunohistochemical labeling for DPC4 mirrors genetic status in pancreatic adenocarcinomas: a new marker of DPC4 inactivation, Am. J. Pathol. 156 (2000) 37–43.
[28] H. Hayashi, T. Higashi, N. Yokoyama, T. Kaida, K. Sakamoto, Y. Fukushima, et al., An imbalance in TAZ and YAP expression in hepatocellular carcinoma confers cancer stem cell-like behaviors contributing to disease progression, Cancer Res. 75 (2015) 4985–4997.
[29] H. Hayashi, T. Higashi, T. Miyata, Y.I. Yamashita, H. Baba, Recent advances in precision medicine for pancreatic ductal adenocarcinoma, Ann. Gastroenterol. Surg. 5 (2021) 457–466.
[30] E.A. Collisson, A. Sadanandam, P. Olson, W.J. Gibb, M. Truitt, S. Gu, et al., Subtypes of pancreatic ductal adenocarcinoma and their differing responses to therapy, Nat. Med. 17 (2011) 500–503.
[31] R.A. Moffitt, R. Marayati, E.L. Flate, K.E. Volmar, S.G. Loeza, K.A. Hoadley, et al., Virtual microdissection identifies distinct tumor- and stroma-specific subtypes of pancreatic ductal adenocarcinoma, Nat. Genet. 47 (2015) 1168–1178.
[32] P. Bailey, D.K. Chang, K. Nones, A.L. Johns, A.M. Patch, M.C. Gingras, et al., Genomic analyses identify molecular subtypes of pancreatic cancer, Nature 531 (2016) 47–52.
[33] C. Jenkinson, V.L. Elliott, A. Evans, L. Oldfield, R.E. Jenkins, D.P. O'Brien, et al., Decreased serum thrombospondin-1 levels in pancreatic cancer patients up to 24 months prior to clinical diagnosis: association with diabetes mellitus, Clin. Cancer Res. 22 (2016) 1734–1743.
[34] X. Qian, V.L. Rothman, R.F. Nicosia, G.P. Tuszynski, Expression of thrombospondin-1 in human pancreatic adenocarcinomas: role in matrix metalloproteinase-9 production, Pathol. Oncol. Res. 7 (2001) 251–259.
[35] S.M. Ribeiro, M. Poczatek, S. Schultz-Cherry, M. Villain, J.E. Murphy-Ullrich, The activation sequence of thrombospondin-1 interacts with the latency-associated peptide to regulate activation of latent transforming growth factor-beta, J. Biol. Chem. 274 (1999) 13586–13593.
[36] S. Wang, Y. Zheng, F. Yang, L. Zhu, X.Q. Zhu, Z.F. Wang, et al., The molecular biology of pancreatic adenocarcinoma: translational challenges and clinical perspectives, Signal Transduct. Target. Ther. 6 (2021) 249.
[37] J. Dardare, A. Witz, J.L. Merlin, P. Gilson, A. Harlé, Smad4 and the TGFβ pathway in patients with pancreatic ductal adenocarcinoma, Int. J. Mol. Sci. 10 (2020) 3534.
[38] M.C. Whittle, K. Izeradjene, P.G. Rani, L. Feng, M.A. Carlson, K.E. DelGiorno, et al., RUNX3 controls a metastatic switch in pancreatic ductal adenocarcinoma, Cell 161 (2015) 1345–1360.
[39] Y.Y. Hsieh, T.P. Liu, C.J. Chou, H.Y. Chen, K.H. Lee, P.M. Yang, Integration of bioinformatics resources reveals the therapeutic benefits of gemcitabine and cell cycle intervention in Smad4-deleted pancreatic ductal adenocarcinoma, Genes 10 (2019) 766 (Basel).
[40] S. Ebbinghaus, M. Hussain, N. Tannir, M. Gordon, A.A. Desai, R.A. Knight, et al., Phase 2 study of ABT-510 in patients with previously untreated advanced renal cell carcinoma, Clin. Cancer Res. 13 (2007) 6689–6695.
[41] A. Molckovsky, L.L. Siu, First-in-class, first-in-human phase I results of targeted agents: highlights of the 2008 American society of clinical oncology meeting, J. Hematol. Oncol. 1 (2008) 20.
[42] A. Prete, A.S. Lo, P.M. Sadow, S.S. Bhasin, Z.A. Antonello, D.M. Vodopivec, et al., Pericytes elicit resistance to vemurafenib and sorafenib therapy in thyroid carcinoma via the TSP-1/TGFbeta1 axis, Clin. Cancer Res. 24 (2018) 6078–6097.
[43] A. Lu, M.A. Pallero, W. Lei, H. Hong, Y. Yang, M.J. Suto, et al., Inhibition of transforming growth factor-beta activation diminishes tumor progression and osteolytic bone disease in mouse models of multiple myeloma, Am. J. Pathol. 186 (2016) 678–690.
[44] J.S. Munger, X. Huang, H. Kawakatsu, M.J. Griffiths, S.L. Dalton, J. Wu, et al., The integrin alpha v beta 6 binds and activates latent TGF beta 1: a mechanism for regulating pulmonary inflammation and fibrosis, Cell 96 (1999) 319–328.
[45] J.P. Annes, J.S. Munger, D.B. Rifkin, Making sense of latent TGF beta activation, J. Cell Sci. 116 (2003) 217–224.
[46] A. Jeanne, C. Schneider, L. Martiny, S. Dedieu, Original insights on thrombospondin-1-related antireceptor strategies in cancer, Front. Pharmacol. 6 (2015) 252.